

Dissipation, topology, and quantum phase transition in a one-dimensional Josephson junction array

Pallab Goswami and Sudip Chakravarty

Department of Physics and Astronomy, University of California Los Angeles, Los Angeles, California 90095-1547, USA

(Received 17 October 2005; published 28 March 2006)

We study the phase diagram and quantum critical properties of a resistively shunted Josephson junction array in one dimension from a strong coupling analysis. After mapping the dissipative quantum phase model to an effective sine-Gordon model we study the renormalization group flow and the phase diagram. We try to bridge the phase diagrams obtained from the weak and the strong coupling renormalization group calculations to extract a more comprehensive picture of the complete phase diagram. The relevance of our theory to experiments in nanowires is discussed.

DOI: [10.1103/PhysRevB.73.094516](https://doi.org/10.1103/PhysRevB.73.094516)

PACS number(s): 74.81.Fa, 68.65.La, 05.30.-d

I. INTRODUCTION

Ohmic dissipation was shown to be of critical importance in the macroscopic quantum coherence of a double-well system.^{1,2} This zero-dimensional problem undergoes a spontaneous symmetry-breaking transition in the ground state if the resistor causing the dissipation is smaller than the quantum of resistance $R_Q = h/4e^2 \approx 6.5 \text{ k}\Omega$; h is the Planck's constant and e the electronic charge. It is perhaps the simplest example of a quantum critical point (QCP).³ Soon afterwards, it was also shown⁴ that a resistively shunted Josephson junction undergoes a similar phase transition from a metallic state (because there is always an ohmic shunt present in the model), in which the phase difference between the superconductors is delocalized, to a superconducting state (in which a supercurrent can flow below the critical current), where the phase difference is localized in a minimum of the cosine potential of the effective classical Hamiltonian derived by Josephson. The root of this remarkable QCP is logarithmic interactions between the instantons⁵ representing the tunneling events, resulting in a dramatic failure of the dilute instanton gas approximation, so successful in the macroscopic quantum tunneling problem.^{6,7} The only difference between the two systems is the specific ordering of the instantons,⁵ but in both cases the underlying cause is the orthogonality catastrophe⁸ of an infrared divergent heat bath that is necessary to model the ohmic shunt resistor. Since then, numerous suggestions have been made that such an essentially dynamic zero temperature ($T=0$) phase transition may be embedded in many condensed matter systems, and this may explain the ubiquity of dissipation in many ultralow temperature phenomena. Instead of enumerating here an incomplete list of references, we refer to Ref. 9.

What about experiments regarding these predictions? We do not merely mean a reduction of the quantum tunneling rate due to dissipation, but a sharp phase transition or a QCP. Surprisingly, experimental evidence is sparse. The closest experiment that indicates symmetry breaking in a double well is an indirect experiment involving a superconducting quantum interference device.¹⁰ In contrast, in a more direct experiment on a single resistively shunted Josephson junction such a dynamic phase transition has been apparently

experimentally observed.¹¹ However, it seems that the theoretical situation is more subtle than that assumed in the past.¹² An attempt to observe such a transition in superconducting nanowires was also made.¹³ Unfortunately, the present experimental situation appears to be unclear.¹⁴⁻¹⁷

Sometimes the simplest theoretical concept is not the simplest from the experimental perspective. From the very beginning it was realized that such a dynamic transition may have important consequences in many body problems,¹⁸⁻²¹ in particular in resistively shunted Josephson junction arrays (RSJJA). Beginning with the pioneering work of Orr *et al.*²² experiments have been few and far in between. A brief recent review is provided by Goldman.²³ Of importance to us here are the experiments of Rimberg *et al.*,²⁴ Takahide *et al.*,²⁵ and Miyazaki *et al.*²⁶ On the theoretical side, many important contributions have been made, but we list here only the papers that are germane to our present work; these are Refs. 27-33.

RSJJA is a simple but nontrivial model, almost a paradigm to use a well-worn word, where both dynamics and statics can simultaneously play an important role in a quantum phase transition, as opposed to a classical phase transition. Compared to a dissipative single junction problem, RSJJA is theoretically more challenging because of the interplay of both spatial and temporal fluctuations. Indeed it is shocking that a recent theoretical work^{34,35} has found that the ground state of RSJJA is a state where the state of the $(0+1)$ -dimensional elements (single Josephson junctions) can slide past each other despite couplings between them. This is despite arbitrarily long-ranged spatial couplings. Such a phase, called the floating phase, was derived from a renormalization group analysis that is perturbative in the Josephson coupling. Given the striking nature of a lower-dimensional quantum criticality embedded in a higher dimensional manifold, it behooves us to examine the phenomena in the strong coupling limit and to see how the two limits are reconciled. From the earlier hints,¹⁹ the strong coupling analysis should show that when the Josephson coupling is gradually increased, the quantum phase transition changes its nature and ceases to be entirely dynamic—topology, quantum mechanics, dissipation, and the collective nature of the problem, all become equally important unlike the weak

coupling limit. Motivated by the theoretical challenge, recent experiments, and the paradigmatic nature of RSJJA, we analyze it in one dimension from the strong coupling limit. As the conceptually important issues are already present in the one-dimensional case, there is no need to examine more complicated higher dimensional situations.

We use Villain mapping to investigate the strong coupling phase diagram and the critical properties. Villain mapping has been used previously to map the phase slip processes to a neutral gas of charges that have anisotropic logarithmic interactions in imaginary time and spatial directions because of dissipation.^{28,29,32,33} We improve upon the previous work and show that the resulting phase diagram is remarkably different. In a Josephson junction array in the absence of dissipation, quantum phase slips are the topological excitations whose classical counterparts are vortices of the classical XY model. One of the basic concepts behind this mapping is a conservation law. Due to tunneling, the number of Cooper pairs will change on the superconducting grains. In the absence of any source or a sink this leads to a continuity equation on the lattice which serves as a constraint on the integer tunneling current. This constraint is resolved in terms of a single integer field defined on a dual space-time lattice, resulting in familiar vortices. Thus the superconductor-insulator transition due to unbinding of vortices can be described by a one-component sine-Gordon model. The presence of shunt resistances, or dissipation, alters this picture. Since we need to include the current through the shunts in addition to the tunneling current, we get a different conservation law with a source term. (This point was missed in the past.) The presence of the source term does not allow us to resolve the current constraint in terms of a single integer field on the dual lattice, and we are left with a neutral gas of two-flavored charges and anisotropic long-range interactions in space time. Consequently, our phase diagram is different from those derived in the past.

The renormalization group equations are obtained by mapping the two-component neutral charge gas system to a two-component sine-Gordon model. A two-component sine-Gordon model was used previously by Refael *et al.* in the context of two resistively shunted Josephson junctions.³⁶ There are therefore some similarities in the phase diagrams. Apart from fully superconducting and metallic states some partially ordered phases are found. Surprisingly, the two-component sine-Gordon model also arises in the context of a classical two-dimensional XY model in the presence of an in-plane magnetic field.³⁷ The magnetic field spoils the zero divergence condition by introducing a source term. Though it is clear that RSJJA and the XY model in an in-plane magnetic field describe different physics, there are some similarities between the RG analyses of both problems.

Our paper is organized as follows. In Sec. II we describe the microscopic model and provide briefly the weak coupling results. In Sec. III we perform a detailed strong coupling analysis employing Villain mapping. To perform RG calculations we map the two flavored neutral charge gas problem arising from Villain mapping to a two-component sine-Gordon model. In Sec. IV we describe the fixed point analysis of the RG recursion relations. In Sec. V we construct the strong coupling phase diagram and contrast the results with

those of the previous authors. In Sec. VI we briefly mention the relation between a superconducting nanowire and a RSJJA. Finally we summarize our results in Sec. VII. We present all the technical details of the RG calculations for the two component sine-Gordon model in the Appendix. Although this is relegated to the Appendix to preserve a smooth flow of the text, this Appendix is the heart of our theoretical work.

II. THE MODEL

We consider the quantum action given by

$$S = \int_0^\beta d\tau \sum_i \frac{\dot{\theta}_i^2}{2E_0} + \frac{\beta\alpha}{4\pi} \sum_{i,n} |\omega_n| |\partial_x \theta_i(n)|^2 - \int_0^\beta d\tau V \sum_i \cos(\partial_x \theta_i). \quad (1)$$

β is the inverse temperature, $E_0 = 2e^2/C$ is the charging energy, where C is the capacitance of a single island. ω_n is the Matsubara frequency and $\alpha = h/4e^2R$ is the dissipation strength, where R is the shunt resistance. $\partial_x \theta_i = \theta_i - \theta_{i+1}$, and V is the Josephson coupling between the grains.

In the weak coupling regime ($\frac{V}{E_0} \ll 1$), which is dominated by strong quantum fluctuations, RG calculations lead to the following recursion relations up to order $O(V^2)$

$$\frac{dV}{dl} = \left(1 - \frac{1}{\alpha}\right)V, \quad \frac{d\alpha}{dl} = 0. \quad (2)$$

So, $\alpha=1$ is a fixed line in the weak coupling limit. For $\alpha > 1$, the system is ordered (superconducting), and V is a relevant operator. For $\alpha < 1$ the system is disordered (metallic), and V is irrelevant. Recently Tewari *et al.*^{34,35} have extended this calculation to the order $O(V^3)$ and have shown that for a one-dimensional array the above set of RG equations are correct up to third order. They also demonstrated that including longer ranged couplings that when V is irrelevant all longer range Josephson couplings are also irrelevant. They become simultaneously relevant with V when $\alpha > 1$. So, around the critical line $\alpha=1$, the chain of Josephson junctions decouples and behaves as independent single junctions. For these reasons the disordered phase (metallic) has been characterized as a floating phase. It is important to understand how far in the $V-\alpha$ plane is this weak coupling RG picture valid.

III. A STRONG COUPLING ANALYSIS

In the strong coupling limit, that is $V/E_0 \gg 1$, the phase difference between the neighboring grains will be localized around the minima of the periodic cosine potential and the tunneling events between the minima will govern the low energy physics. We analyze these tunneling events using Villain mapping. To employ Villain mapping we first discretize

the imaginary time into N slices so that $\beta=N\Delta\tau$ where $\Delta\tau$ is the lattice spacing in imaginary time direction. After discretizing, the partition function becomes

$$Z = \int [D\theta] \exp \left[J_\mu \sum_{\vec{l}} [1 - \cos \nabla_\mu \theta(\vec{l})] - \sum_{\vec{q}} \frac{\alpha}{4\pi} |\omega| \Delta\tau f(k) |\theta(\vec{q})|^2 \right], \quad (3)$$

where the summation over repeated indices is implied. $\mu \equiv (\tau, x)$ represents the components on the space-time lattice and \vec{l} stands for the space-time coordinates of the lattice points. Here $J_\tau = 1/E_0 \Delta\tau$, $J_x = V \Delta\tau$, and $f(k) = 2[1 - \cos(ka)]$. For both J_τ and J_x large we can replace the cosine by a periodic Gaussian, as follows:

$$Z = \int [D\theta] \sum_{m_\mu(\vec{l})} \exp \left[-\frac{J_\mu}{2} \sum_{\vec{l}} [\nabla_\mu \theta(\vec{l}) - 2\pi m_\mu(\vec{l})]^2 - \sum_{\vec{q}} \frac{\alpha}{4\pi} |\omega| \Delta\tau f(k) |\theta(\vec{q})|^2 \right]. \quad (4)$$

Here $m_\mu(i, \tau)$ are integers and represent tunneling between minima of the cosine potential.

Before we proceed further with the action described by Eq. (4), we explicitly demonstrate the difference of the conservation laws in nondissipative and a dissipative Josephson junction array as have been mentioned in the Introduction. First we choose the nondissipative case, and we set $\alpha=0$ in Eq. (4). We also introduce two auxiliary fields B_μ to decouple the periodic Gaussian terms as

$$Z \propto \int [D\theta][DB_\mu] \sum_{m_\mu(\vec{l})} \exp \left[-\sum_{\mu, \vec{l}} \left(\frac{B_\mu^2(\vec{l})}{2J_\mu} + iB_\mu(\vec{l}) \times [\nabla_\mu \theta(\vec{l}) - 2\pi m_\mu(\vec{l})] \right) \right]. \quad (5)$$

Summation over the integer field m_μ restricts the continuous fields B_μ to integer values and integrating out θ we obtain

$$Z \propto \sum_{B_\mu} \delta_{\nabla_\mu B_\mu, 0} \exp \left[-\sum_{\mu, \vec{l}} \frac{B_\mu^2(\vec{l})}{2J_\mu} \right]. \quad (6)$$

So, we obtained the conservation law $\nabla_\mu B_\mu = 0$ in the form of a constraint on the configurations of B_μ . If we choose $B_x = \partial_\tau h$, $B_\tau = -\partial_x h$ where h is a single component integer field the constraint is resolved. For any nonzero α , we introduce an additional auxiliary field ρ to decouple the quadratic dissipative term:

$$\begin{aligned} & \exp \left[-\sum_{\vec{q}} \frac{\alpha}{4\pi} |\omega| \Delta\tau f(k) |\theta(\vec{q})|^2 \right] \\ &= \int [D\rho] \exp \left[-\sum_{\vec{q}} \frac{|\rho(\vec{q})|^2}{\left[\frac{\alpha}{4\pi} |\omega| \Delta\tau f(k) \right]} + i \sum_{\vec{l}} \rho(\vec{l}) \theta(\vec{l}) \right]. \end{aligned} \quad (7)$$

Now integrating out θ we obtain the modified conservation law

$$\nabla_\mu B_\mu + \rho = 0 \quad (8)$$

which directly demonstrates that the zero divergence condition is destroyed and the auxiliary field ρ serves as a source term.

We proceed with an analysis of Eq. (4). Integrating out θ from the partition function and doing the following transformations,

$$p_1(i, \tau) = m_\tau(i+1, \tau) - m_\tau(i, \tau), \quad (9)$$

$$p_2(i, \tau) = m_x(i, \tau + \Delta\tau) - m_x(i, \tau), \quad (10)$$

we obtain

$$Z = Z_{SW} \sum_{p^\mu(\vec{l})} \exp \left[-2\pi^2 \sum_{\vec{q}} p^\mu(\vec{q}) G_{\mu, \nu}(\vec{q}) p^\nu(-\vec{q}) \right]. \quad (11)$$

In the above step we have rescaled time direction as $\Delta\tau' = \Delta\tau \sqrt{VE_0} a$. So, we have rewritten the partition function in terms of two kinds of interacting charges p_1 and p_2 which by construction form a neutral gas of charges. Interactions of the charges are encoded in the $G_{\mu, \nu}(\vec{q})$ which are given by

$$G_{11}(k, \omega') = \frac{J}{\Delta\tau' a (k^2 + \omega'^2)} + \frac{\alpha}{2\pi \Delta\tau'} \frac{|\omega'|}{(k^2 + \omega'^2)}, \quad (12)$$

$$\begin{aligned} G_{22}(k, \omega') &= \frac{J}{\Delta\tau' a (k^2 + \omega'^2)} + \frac{\alpha}{2\pi \omega' \Delta\tau'} \\ &\quad - \frac{\alpha}{2\pi \Delta\tau'} \frac{|\omega'|}{(k^2 + \omega'^2)}, \end{aligned} \quad (13)$$

$$G_{12}(k, \omega') = -\frac{J}{\Delta\tau' a (k^2 + \omega'^2)} = G_{21}. \quad (14)$$

In the long-wavelength and low-frequency limit,

$$G_{ij} = (-1)^{i+j} \frac{J}{\Delta\tau' a (k^2 + \omega'^2)} + \delta_{i,2} \delta_{j,2} \frac{\alpha}{2\pi \omega' \Delta\tau'}, \quad (15)$$

where $J = \sqrt{J_x J_\tau} = \sqrt{V/E_0}$. From this interaction matrix it becomes clear that because of dissipation spatial kinks, i.e., p_2 , have an additional anisotropic on-site logarithmic interaction in imaginary time in addition to isotropic logarithmic interaction in space time. Charges of opposite sign for a given flavor attract and for different flavors charges of same sign attract. In the presence of dissipation we cannot reduce the partition function in terms of a single set of charges or vortices given by $p_3 = p_2 - p_1 = \epsilon_{\mu\nu} \partial_\mu m_\nu$. So, we have to work

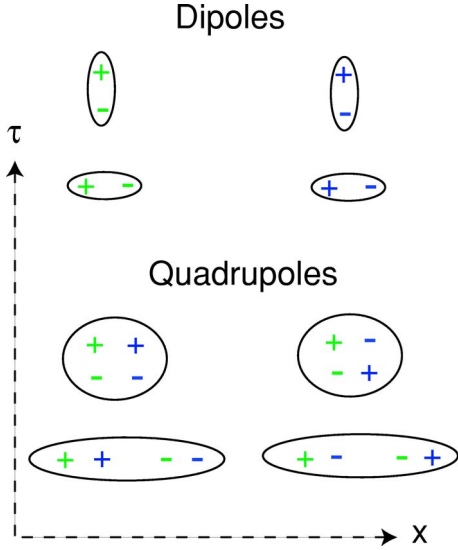


FIG. 1. (Color online) Configurations of space-time dipoles and quadrupoles of different flavors. Note that equivalent pictures can be drawn by charge conjugations.

with a two-component neutral charge gas, and the corresponding sine-Gordon theory will be a two-component field theory. For convenience we shall choose $\Delta\tau = 1/\sqrt{VE_0}$, which leads to $\Delta\tau' = a$. With this choice, the space-time lattice becomes isotropic and the anisotropy of the problem is captured only through the anisotropy of the interaction terms.

We introduce two fugacities y_1, y_2 corresponding to p_1, p_2 to control the charge fluctuations. As usual, for small y_1, y_2 we can restrict p_1, p_2 to $0, \pm 1$. Thus the sine-Gordon action is

$$S = \frac{1}{2} \sum_{k, \omega} \vec{\phi}^* \tilde{G}^{-1} \vec{\phi} - \sum_{i=1}^2 \frac{2y_i}{a^2} \int d\vec{x} \cos(2\pi\phi_i) - \sum_{\pm} \frac{2y_{\pm}}{a^2} \int d\vec{x} \cos(2\pi\phi_1 \pm 2\pi\phi_2). \quad (16)$$

We are using the vector notation $\vec{x} = (x, \tau)$ and $\int d\vec{x} = \int dx d\tau$. y_+, y_- are combinations of y_1, y_2 . At second order in fugacities, the RG procedures generate $\cos(2\pi\phi_1 \pm 2\pi\phi_2)$ terms, and that is the reason for extending the coupling constant space. y_i controls the formation dipoles between different signs of charges for i th flavor. When the charges are bound as dipoles, the fugacities become irrelevant and flow to zero, implying order; when they become relevant free charges proliferate. y_+ controls the density of dipoles between charges of same sign but of different flavors, and y_- controls the density of dipoles between charges of opposite sign and different flavors; see Fig. 1. \tilde{G}^{-1} is the matrix inverse of the interaction matrix for the charges. This 2×2 matrix is given by

$$G_{ij}^{-1} = \delta_{i,1} \delta_{j,1} \frac{k^2 + \omega^2}{J} + \frac{2\pi}{\alpha} |\omega|. \quad (17)$$

Interestingly, the presence of the divergent $\frac{1}{|\omega|}$ term in the propagator requires that we formulate the RG (thinning out the degrees of freedom) by integrating only in a given fre-

quency shell. Then a dimensional analysis with the scaling prescription $k \rightarrow ke^{-l/z}$, $\omega \rightarrow \omega e^{-l}$, where l is the length rescaling factor, shows that

$$\frac{d\alpha}{dl} = 0, \quad (18)$$

as α is dimensionless. Since $|\omega|$ is nonanalytic and we have to maintain the periodicity of the cosine terms, the above RG equation for α is exact.^{38,39} The following recursion relations up to second order are derived in the Appendix:

$$\frac{dy_1}{dl} = \left(1 + \frac{1}{z} - \pi J\right) y_1 + \alpha y_2 y_+ + (2\pi J + \alpha) y_2 y_-, \quad (19)$$

$$\frac{dy_2}{dl} = \left(1 + \frac{1}{z} - \pi J - \alpha\right) y_2 + 2\pi J y_1 y_-, \quad (20)$$

$$\frac{dy_+}{dl} = \left(1 + \frac{1}{z} - \alpha\right) y_+ + \pi J y_1 y_2, \quad (21)$$

$$\frac{dy_-}{dl} = \left(1 + \frac{1}{z} - 2\pi J - \alpha\right) y_- - \pi J y_1 y_2, \quad (22)$$

$$\frac{dJ}{dl} = J \left[\left(1 - \frac{1}{z}\right) - J(A_1 y_1^2 + A_+ y_+^2 + A_- y_-^2) \right]. \quad (23)$$

To keep the coefficient of k^2 fixed we need

$$\frac{1}{z} = 1 - \frac{A_+ y_+^2}{2}. \quad (24)$$

Here A_1, A_+ , and A_- are regularization dependent constants.

IV. THE FIXED POINTS

From first order RG equations, the following picture emerges: $\frac{1}{z} = 1$ and the entire $J - \alpha$ plane is broken into six regions. In the region $\pi J > 2$, $\alpha > 2$ all the fugacities are irrelevant, and the system is fully superconducting and in the region $(4\pi J + \alpha < 2)$ all the fugacities are relevant, and the system is fully metallic. The other four regions are mixed phases where one or more fugacities become relevant thus implying special kinds of charge proliferation processes. These four phases therefore have partial or mixed order.

To find the fixed points of the second order equations, we first note the structure of the equation for y_+ . Since all the fugacities and J are always positive, when $1 + \frac{1}{z} - \alpha > 0$, y_+ and $J y_1 y_2$ have to be zero. For Lorentz invariant fixed points corresponding to $\frac{1}{z} = 1$ and the coupling constant space specified by $1 + \frac{1}{z} - \alpha > 0$, which we can also write as $A_+ y_+^2 / 2 + \alpha < 2$, we find the following fixed point solution:

$$\text{FP1: } y_1 = y_2 = y_+ = y_- = 0, \quad J = J^*, \quad \alpha = \alpha^* < 2. \quad (25)$$

When $1 + \frac{1}{z} - \alpha < 0$, i.e., $A_+ y_+^2 / 2 + \alpha > 2$, we get

$$\text{FP2: } y_1 = y_2 = y_+ = y_- = 0, \quad J = J^*, \quad \alpha = \alpha^* > 2. \quad (26)$$

It is interesting to note that FP2 also corresponds to $\frac{1}{z} = 1$. It is also worth emphasizing FP1 and FP2 describe different

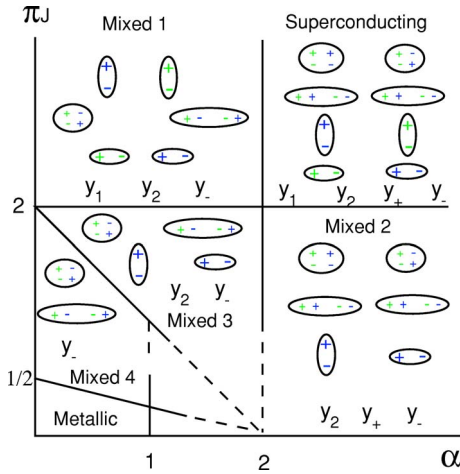


FIG. 2. (Color online) Phase diagram. Other than fully metallic and superconducting phases, there are four mixed phases characterized by the fugacities that are irrelevant. The strong coupling phase diagram should not be valid for $\pi J \ll 1$. The local critical boundary at $\alpha = 1$, at weak coupling, requires a separate analysis, as described in the text.

parts of the J - α plane. They are not critical points; there are lines of critical points in the surfaces containing these fixed points, which are the same as those found from the first order RG equations.

Consider now $1 + \frac{1}{z} - \alpha = 0$. For the results to be sensible, z must be positive and therefore $\alpha > 1$. The fixed points are now non-Lorentz invariant, and they are given by

$$\text{FP3: } y_1^* = y_2^* = y_-^* = 0, \quad J^* = 0, \quad A_+ y_+^{*2} + 2\alpha^* = 4, \quad (27)$$

$$\text{FP4: } y_1^* = y_2^* = y_-^* = 0, \quad A_+ y_+^{*2} + 2\alpha^* = 4, \quad J^* = \frac{1}{2}, \quad (28)$$

$$\text{FP5: } y_2^* = y_-^* = 0, \quad A_+ y_+^{*2} + 2\alpha^* = 4, \quad J^* = \frac{\alpha^*}{\pi},$$

$$y_1^{*2} = \frac{(2 - \alpha^*)(\pi - 2\alpha^*)}{A_1 \alpha^*}, \quad 1 < \alpha^* < \frac{\pi}{2}. \quad (29)$$

These three sets of fixed points have continuously varying dynamic scaling exponents. However, despite the presence of nonuniversal constants, z is universally determined by α^* . The only nonuniversality is in the location of the fixed points. Importantly FP4 and FP5 are the sought after intermediate coupling fixed points controlling the crossover between the local criticality and the global criticality, which are not accessible in weak coupling calculations.

V. THE PHASE DIAGRAM

In this section we construct the phase diagram, which is determined by FP1 and FP2. This is illustrated in Fig. 2. In the region, $(\pi J > 2, \alpha > 2)$, all the fugacities are irrelevant and hence this phase is fully superconducting and is labeled

as superconducting. Here, each flavor of charges are bound in dipoles and the dipoles are formed between charges of opposite sign. Also, y_+ is irrelevant, implying a quadrupolar order: dipoles formed between two different flavors of charges, but of the same sign, are controlled by y_+ and hence in this region the interflavor dipoles are bound in quadrupoles. Following the similar argument for y_- , we can conclude that interflavor dipoles formed between charges of different flavors and opposite signs are bound as quadrupoles. These different dipolar and quadrupolar orders are shown in Fig. 2. In the region, $(4\pi J + \alpha < 2)$, all the fugacities, y_1, y_2, y_+, y_- are relevant, and this is fully disordered or the metallic phase. Both flavors of charges proliferate and also the interflavor dipoles proliferate and we label this as metallic. In the region, $(\pi J > 2, \alpha < 2)$, only y_1, y_2, y_- are irrelevant and only y_+ is relevant. This implies that each flavor of charges exhibits dipolar order but interflavor dipoles controlled by y_+ proliferate. Hence this is a mixed phase. This phase is labeled as mixed 1. So, the transition between the phases mixed 1 and superconducting is between a dipole gas and quadrupolar order. In the region, $(\pi J < 2, \alpha > 2)$, p_2 charges are bound in dipoles and there is also quadrupolar order. But, p_1 charges proliferate. These facts are reflected by the irrelevance of y_2, y_+, y_- and the relevance of y_1 . For this reason this is a phase of mixed order and we label this as mixed 2. In the region, $(\pi J + \alpha > 2, \pi J < 2, \alpha < 2)$, y_2, y_- are irrelevant, and y_1, y_+ are relevant. p_2 charges are bound in dipoles and interflavor dipoles controlled by y_- are bound as quadrupoles. But both the p_1 charges as well as the interflavor dipoles controlled by y_+ proliferate, which is also an example of mixed order. This region is labeled as mixed 3. In the region, $(4\pi J + \alpha > 2, \pi J + \alpha < 2)$, only y_- is irrelevant and all other fugacities are relevant. So, interflavor dipoles controlled by y_- are bound as quadrupoles but p_1, p_2 charges and interflavor dipoles controlled by y_+ proliferate. This is also an example of mixed order and is labeled as mixed 4.

VI. CONCLUSIONS

In this section we note our observations in regard to the recent weak coupling analysis of the floating phase and briefly describe the relevance of our theoretical work to various experiments that we have alluded to in the Introduction. In the near future, we hope to fully discuss the experimental consequences of our theory. For nanowires, a number of important issues need to be addressed, such as the effect of the external circuit for short wires, dissipative effects due to external circuit and the resistance of the phase slip cores, boundary effects due to the leads,^{36,40-42} and inhomogeneities.¹⁶ For experiments involving arrays, the real time dynamics and the current-voltage characteristics would be a major theoretical project. Presently, we can make only qualitative remarks that follow from our thermodynamic phase diagram.

A. Floating phase and the local quantum criticality

From the RG calculations at the second order, we found that $1/z$ depends on the fugacity y_+ . Therefore the locations

of the nontrivial fixed points FP3, FP4, and FP5 found above depend on y_+ . These fixed points can be accessed by tuning of y_+ , in addition to tuning J and α . This is the reason why they do not appear in the phase diagram, which is a cut in the J - α plane. To recover the local quantum criticality observed in the weak coupling limit we note that as J is decreased below $2/\pi$, the fugacity y_1 becomes relevant, and we can no longer use the flows derived from small fugacity expansions after a certain value of J . However, we observe that the growth of y_1 implies that p_1 charges proliferate, and this fact allows us to restrict $\phi_1 \approx 0$. Because of the anisotropic imaginary time interaction, p_2 charges may not proliferate at the same time. Using this approximation, the two-component sine-Gordon problem reduces now to a one-component sine-Gordon problem described by the action

$$S \approx \frac{1}{2} \sum_{k,\omega} \frac{2\pi}{\alpha} |\omega| |\phi_2|^2 - 2 \frac{y_2}{a^2} \int d\vec{x} \cos(2\pi\phi_2). \quad (30)$$

Since the propagator depends now only on $|\omega|$, the problem is effectively zero dimensional. Note that this action by itself has an approximate duality with the weak coupling action in terms of the junction variables $\psi_i = \theta_i - \theta_{i+1}$ under the identification $y_2 \rightarrow V$ and $\alpha \rightarrow 1/\alpha$. The self-duality at $\alpha=1$ is identical to the single junction problem. Thus, as the weak coupling limit is approached, at an intermediate coupling strength there is a change in the behavior from a global criticality to a local criticality. This can be easily recognized from the lack of self-duality of the Josephson junction chain. By a simple RG calculation we will get

$$\begin{aligned} \frac{dy_2}{dl} &= (1 - \alpha)y_2, \\ \frac{d\alpha}{dl} &= 0. \end{aligned} \quad (31)$$

If $\alpha > 1$, y_2 becomes irrelevant implying ordered state and as $\alpha < 1$ the system becomes disordered. Here the ordering is a local ordering of the individual junctions.

B. Josephson junction array

In this section we describe the relevance of our theoretical analysis regarding the experiments on resistively shunted Josephson junction arrays in one dimension. We have found that the phase boundary between superconducting and fully metallic phase depends on the strength of the Josephson coupling of the superconducting grains. In our analysis we have predicted a complicated phase diagram involving mixed phases in addition to fully superconducting and fully metallic states, depending on the strength of J . Only two transitions (between mixed 1 and superconducting and between mixed 2 and mixed 3) take place which are independent of the strength of J . The experimentally determined phase diagram due to Miyazaki *et al.*²⁶ confirms the strong coupling prediction that the phase boundary between ordered and disordered phase depends on J and it also shows that in the weak coupling limit there is a part of the phase boundary at $\alpha=1$ which is independent of J . More detailed experiments are

necessary to establish the complete phase diagram on a quantitative level for the entire J - α plane and would be possible when we establish the signature of many of the mixed phases, which are mainly dynamical.

Apart from the region in which the system is fully metallic, all other regions correspond to either fully superconducting or mixed phases. We expect these superconducting and mixed phases to demonstrate power law behaviors for the temperature dependence of zero bias resistance: different mixed phases and the fully superconducting phase can be distinguished by their different temperature exponents. Similar power law behaviors are also expected for the I - V characteristic. These power law exponents will depend on J and α which can be inferred from the linearized RG equations about the fixed points.

C. Superconducting nanowires

There is also a broad relevance of the dissipative Josephson junction array in the context of the experiments on superconducting nanowires.¹³⁻¹⁷ At $T=0$ quantum phase slips should play the key role in determining if the system will be superconducting or resistive. An experiment by Bezryadin *et al.*¹³ on a superconducting nanowire observed a dissipative phase transition similar to a single junction problem when the total normal resistance of the wire R_N exceeded R_Q . Later work¹⁴ implied that it is rather the resistance per unit length, hence the diameter of the wire, that is of significance.

Quantum phase slips are topological excitations in which the phase of the superconducting order parameter slips by a quantized amount and can be viewed as a vortex in the space-time manifold at $T=0$. If, for the moment, we can ignore dissipation and model the wire at $T=0$ as a $(1+1)$ -dimensional XY model, it is well-known that such a system cannot exhibit a sharp phase transition (Kosterlitz-Thouless) without consideration of topology or vortex unbinding; smooth Gaussian fluctuations, "spin waves," cannot destroy superconductivity. The finite temperature properties in the proximity of the QCP can be understood in terms of universal scaling functions, and for a finite wire, a finite size scaling analysis becomes necessary.

For a quantum system, the above picture must be modified because statics and dynamics are intricately intertwined. So, one must specify an appropriate dynamical model. In one such model Cooper pairs are allowed to disappear in a pool of normal electrons.⁴⁰ Thus it is the actual phase of a superconducting grain that is coupled to an ohmic heat bath. While this may be sensible for a system of superconducting grains embedded in a normal metal,^{43,44} it does not seem to reflect the physical situation in a superconducting nanowire.

The RSJJA is another model for a superconducting nanowire, at least as far as the global $T=0$ phase diagram is concerned. The Josephson energy V provides an energy barrier for phase slips for currents up to the critical current, and the topological excitations that are so essential are automatically built in the model. At a coarse grained level, on the scale of a coherence length ξ , we can think of the wire to be partitioned into superconducting segments interrupted by the cores of the phase slips forming Josephson junctions. The

characteristic frequency of the phase slips is given by the gap at which the conductivities of the normal metal and the superconductor are the same. So, the system will have three coupling constants α , E_0 , and V corresponding to the degree of dissipation, the charging energy of the grains, and the Josephson coupling strength. Here, the dissipation strength $\alpha = R_Q/R_\xi$ and $R_\xi = \rho\xi/\pi r^2$, where ρ is the resistivity and r is the wire radius. Importantly, we believe that the correct model for the dissipative coupling is the one in which the phase *difference* across the phase slip is coupled to an ohmic heat bath, as for RSJJA, unlike the model of Ref. 40.

To determine the charging energy and the Josephson coupling strength, we consider the continuum action that describes the Mooij-Schön⁴⁵ mode (gapless plasmon mode arising out of incomplete screening in one dimension) and is given by

$$S = \frac{\mu}{2\pi} \int_0^\beta d\tau \int_{-L/2}^{L/2} dx \left[c_s (\partial_x \phi)^2 + \frac{1}{c_s} (\partial_\tau \phi)^2 \right], \quad (32)$$

where μ and c_s are the dimensionless kinetic admittance of the superconducting nanowire and the speed of propagation of the plasmon mode, respectively. We have set $\hbar=1$. μ and c_s are related to the superfluid density and the capacitance of the wire by the relations $\frac{\mu c_s}{2\pi} = \frac{\rho_s}{2} = \frac{n_s A}{4m}$ and $\frac{\mu}{2\pi c_s} = \frac{\tilde{C}}{8e^2}$. A is the cross section, \tilde{C} is the capacitance per unit length, and n_s the bulk superfluid density. If we discretize this action on the scale of a lattice spacing a , of the order of the superconducting coherence length ξ , we get the action of a Josephson junction chain with its parameters fixed by those of the Mooij-Schön mode. For the Josephson junction chain we get the following coupling constant relations: $V = \frac{\mu c_s}{\pi a}$ and $\frac{\mu a}{c_s} = \frac{1}{E_0}$. For the strong coupling limit of the Josephson junction array the dimensionless parameter $J = \mu/\pi$. If we define kinetic inductance per unit length of the wire as $\tilde{L} = 1/e^2 \rho_s$ we get $\mu = R_Q/\sqrt{\tilde{L}/\tilde{C}}$. Kinetic inductance per unit length can be expressed in terms of London penetration depth λ_L as $\tilde{L} = \frac{\mu_0 \lambda_L^2 \xi}{Al_0}$ where l_0 is the mean free path of the electrons. Converting this in terms of the normal resistance per unit length of the wire \tilde{R} we get $\tilde{L} \approx \frac{\hbar \tilde{R}}{1.76 \pi k_B T_c}$ where we have restored \hbar .

We should note that, to leading order, we have $J \propto r$, as the capacitance per unit length has only a weak logarithmic dependence on r . So, a phase transition dependent on J or μ implies a dependence on the radius of the wire, that is, it tells us a critical radius beyond which superconductivity can be destroyed and these facts are in qualitative agreement with the results of Zaikin *et al.*⁴⁶ and Refs. 41 and 42. This fact is also in qualitative agreement with the experimental results when the resistance per unit length is plotted against the temperature.¹⁴ In recent experiments on single-crystal Sn nanowires, Tian *et al.*¹⁷ have also emphasized the role of the diameter of the wire for very low temperature measurements, well below T_c .

Up to now it might seem that there are no differences between our results and those of Zaikin *et al.* and Büchler *et al.* If we go through the data of Lau *et al.*¹⁴ carefully, we will find that for the MoGe wires used in the experiments $\alpha > 2$.

So, in these experiments only control parameter is dimensionless admittance. This is the reason why our quantitative prediction $\mu=2$ is the same. But, significant differences will arise if the diameter and other system parameters can be adjusted such that $\alpha < 2$; in this regime, we will observe transitions between the mixed phases and also between the metallic and the mixed phases, depending on the coupling strengths. In the mixed phases, the resistance will follow various power laws as a function of temperature. For $\alpha < 2$, these exponents will depend on both μ and α in contrast to the situation when $\alpha > 2$, where the exponent depends only on μ . So, only if α as well as μ can be made sufficiently small, a local quantum criticality can be observed. Prediction of the transitions is the outcome of treating the wire as an effective RSJJA and we believe can be verified in a more elaborate set of experiments on thinner wires and different materials.

Before concluding this section we should mention that we did not take into account a few effects. One is the boundary effects due to the leads^{36,40-42} and the second is the possibility of inhomogeneities resulting in weak links. That inhomogeneities can play an important role is evident from the recent experiments of Bollinger *et al.*¹⁶ Another experimentally relevant issue is the effect of disorder on quantum phase slips. In a recent paper Khlebnikov and Pryadko⁴⁷ considered the effect of disorder and demonstrated that disorder can bind the spatial coordinates of the phase slips and antiphase slips and hence convert the problem to an effective (0+1)-dimensional problem. They found that the phase transition takes place at $\mu=1$ and belongs to the dissipative universality class which we have defined to be the local quantum criticality. We hope to return to these interesting effects relevant to the experiments in a future work.

ACKNOWLEDGMENTS

We thank M. Tinkham for discussions. A part of this work was carried out by one of us (S.C.) at the Aspen Center for Physics during the summer workshop ‘‘Coherence and Dissipation in Quantum Systems’’ in 2004. This work was supported by a grant from the National Science Foundation: NSF-DMR 0411931.

APPENDIX: THE DERIVATION OF THE RENORMALIZATION GROUP EQUATIONS

In the small fugacity limit we can expand the partition function in powers of fugacities and truncate at the quadratic order. If ϕ_i has frequency and momentum components in the shell $a^{-1}e^{-l} < \omega < a^{-1}$ and $a^{-1}e^{-llz} < k < a^{-1}$, we define it to be the fast mode, ϕ_i^f ; otherwise, a mode is defined to be slow ϕ_i^s . For a fixed frequency shell, we integrate out the momenta, and then rescale both frequency and momentum in the resulting action for the slow part (see Fig. 3). The dynamic exponent z is necessary to capture the effects of the anisotropic interaction. The reason for this special order of integration is because of $1/|\omega|$ in the propagator for ϕ_2 . If we reversed the order of integration, we would have encountered spurious infrared divergence from the frequency integration.

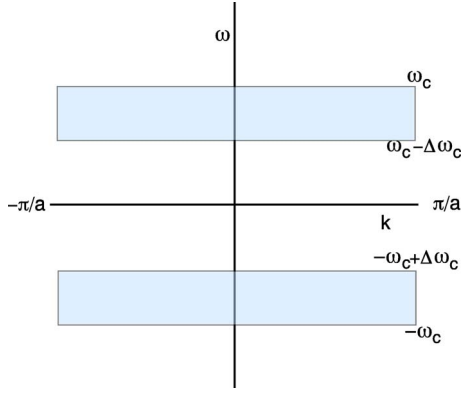


FIG. 3. (Color online) Renormalization group shell integration. The integration proceeds by integrating out the shaded areas.

While rescaling we must maintain the periodicity of the cosine terms, which implies that the field renormalization constant is unity. Cosine averages are being calculated with respect to the fast degrees of freedom being integrated out and it is denoted as $\langle \cdots \rangle^f$. For any operator $O[\phi_1, \phi_2]$, the average $\langle O \rangle^f$ is defined as

$$\langle O \rangle^f = \int D[\vec{\phi}^f] \exp[-S[\vec{\phi}^f]] O[\phi_1, \phi_2]. \quad (\text{A1})$$

We then arrive at the following action for the slow degrees of freedom:

$$\begin{aligned} \mathcal{S}[\vec{\phi}_s] &= \frac{1}{2} \sum_{k, \omega} \vec{\phi}_s^* \tilde{G}^{-1} \vec{\phi}_s \\ &- \sum_i \frac{2y_i}{a^2} \int d\vec{x} \langle \cos(2\pi\phi_i) \rangle^f \\ &- \sum_{\eta=\pm} \frac{2y_\eta}{a^2} \int d\vec{x} \langle \cos[2\pi(\phi_1 + \eta\phi_2)] \rangle^f - \sum_{i,j=1}^2 I_{ij} \\ &- \sum_{i=1,2, \alpha=\pm} I_{i\alpha} - \sum_{\alpha, \beta=\pm} I_{\alpha\beta}, \end{aligned} \quad (\text{A2})$$

where I_{ij} , $I_{i\alpha}$, and $I_{\alpha\beta}$ represent the following second order contributions:

$$\begin{aligned} I_{i,j} &= \left(\frac{2y_i y_j}{a^4} \right) \int_{\vec{x}_1, \vec{x}_2} \langle \cos[2\pi\phi_i(\vec{x}_1)] \cos[2\pi\phi_j(\vec{x}_2)] \rangle^f, \\ I_{i,\alpha} &= \left(\frac{2y_i y_\alpha}{a^4} \right) \int_{\vec{x}_1, \vec{x}_2} \langle \cos[2\pi\phi_1(\vec{x}_2) + 2\pi\alpha\phi_2(\vec{x}_2)] \\ &\quad \times \cos[2\pi\phi_i(\vec{x}_1)] \rangle^f, \\ I_{\alpha,\beta} &= \left(\frac{2y_\alpha y_\beta}{a^4} \right) \int_{\vec{x}_1, \vec{x}_2} \langle \cos[2\pi\phi_1(\vec{x}_1) + 2\pi\alpha\phi_2(\vec{x}_1)] \\ &\quad \times \cos[2\pi\phi_1(\vec{x}_2) + 2\pi\beta\phi_2(\vec{x}_2)] \rangle^f. \end{aligned} \quad (\text{A3})$$

As previously used in the text, we are using the vector notation $\vec{x} = (x, \tau)$ and $\int_{\vec{x}} = \int dx d\tau$. The calculation involves the propagators $G_{ij}^f(x_2 - x_1, \tau_2 - \tau_1) \equiv G_{ij}^f(\vec{x}_2 - \vec{x}_1) = G_{ij}^f(\vec{r})$,

which has an oscillatory behavior for long distance due to the sharp cutoff in frequency. With suitable regularization we can avoid the complications that can arise due to this oscillatory behavior. Different regularizations lead to different nonuniversal constants in the recursion relations, but they do not affect the universal properties. We use the following regularized propagators:

$$G_{11}^f(\vec{r}) = \frac{J}{2\pi} K_0(\lambda \sqrt{|\vec{r}|^2 + a^2}) = -G_{12}^f(\vec{r}) = -G_{21}^f(\vec{r}) \quad (\text{A4})$$

and

$$G_{22}^f(\vec{r}) = \delta(x) \frac{\alpha}{2\pi^2} K_0(\lambda \sqrt{\tau^2 + a^2}) + \frac{J}{2\pi} K_0(\lambda \sqrt{|\vec{r}|^2 + a^2}),$$

where $\lambda = a^{-1} e^{-l}$. K_0 is the modified Bessel function. For distance much greater than the cutoff these regularized propagators fall off exponentially and for distance much less than λ^{-1} they have logarithmic dependence on distance. For example,

$$\begin{aligned} \frac{y_i}{a^2} \int d\vec{x} \langle \cos[2\pi\phi_i(\vec{x})] \rangle^f \\ &= \frac{y_i}{a^2} \int d\vec{x} \langle \cos[2\pi\phi_i^s(\vec{x}) + 2\pi\phi_i^f(\vec{x})] \rangle^f \\ &= \frac{y_i}{a^2} \int d\vec{x} \cos[2\pi\phi_i^s(\vec{x})] \exp[-2\pi^2 \langle \phi_i^2(\vec{x}) \rangle^f] \\ &= \frac{y_i}{a^2} \exp[-2\pi^2 G_{ii}^f(0)] \int d\vec{x} \cos[2\pi\phi_i^s(\vec{x})]. \end{aligned} \quad (\text{A5})$$

After rescaling the coordinates we obtain

$$y_i(l) = \exp\left[\left(1 + \frac{1}{z}\right)l - 2\pi^2 G_{ii}^f(0)\right] y_i(0). \quad (\text{A6})$$

When we compute an average $\langle \cos[2\pi\phi_1(\vec{x}) \pm 2\pi\phi_2(\vec{x})] \rangle^f$ it involves computing the average $\langle [\phi_1(\vec{x}) \pm \phi_2(\vec{x})]^2 \rangle^f$. Due to the mutual interaction between ϕ_1 and ϕ_2 fields we obtain

$$\langle [\phi_1(\vec{x}) \pm \phi_2(\vec{x})]^2 \rangle^f = G_{11}^f(0) + G_{22}^f(0) \pm 2G_{12}^f(0), \quad (\text{A7})$$

which leads to

$$\begin{aligned} y_\pm(l) &= \exp\left[\left(1 + \frac{1}{z}\right)l - 2\pi^2 [G_{11}^f(0) \right. \\ &\quad \left. + G_{22}^f(0) \pm 2G_{12}^f(0)]\right] y_\pm(0). \end{aligned} \quad (\text{A8})$$

From Eqs. (A5) and (A7) we obtain the first order RG equations for the fugacities.

Now we illustrate the calculations of the second order terms. All the second order terms involve two space time coordinates (\vec{x}_1, \vec{x}_2) but the propagators in real space time are only functions of relative space-time coordinate $(\vec{x}_2 - \vec{x}_1)$. For this reason we do a coordinate transformation to the center of mass coordinate $(\vec{R} = \frac{\vec{x}_1 + \vec{x}_2}{2})$ and the relative coordinate $(\vec{r} = \vec{x}_2 - \vec{x}_1)$. The second order contribution I_{11} will involve only

the isotropic propagator $G_{11}^f(|\vec{r}|)$. In order to calculate such a term we can go over to polar coordinates for the relative vector \vec{r} which has the following three ranges:

$$\int d\vec{r} = \int_0^{2\pi} d\theta \left[\int_0^a r dr + \int_a^{ae^l} r dr + \int_{ae^l}^\infty r dr \right]. \quad (\text{A9})$$

In the first range of integration we can take the propagator $G_{11}^f(|\vec{r}|) = G_{11}^f(0)$; in the second range either we can set $G_{11}^f(|\vec{r}|) = G_{11}^f(a)$ or carry out the integral with the regularized logarithmic form of the propagator combined with a gradient expansion of the cosine terms. With suitable regularization, $G_{11}^f(|\vec{r}|)$ can be converted into a short range function of $|\vec{r}|$ and the third part of the integral can be made negligible.^{48,49} The specific regularization controls how fast and how smooth the propagator falls off with the distance but does not affect the universal properties. This is what we achieve with the regularized propagator mentioned above.

Due to the anisotropic part in the propagator G_{22}^f , the above decomposition into polar coordinates can be incorrect for the second order terms involving the field ϕ_2 . So, we have to check all the second order terms mentioned above independently. As we will demonstrate below the second order terms consisting of cross correlation of the fields ϕ_1, ϕ_2 lead to integrals over combination of G_{11}^f, G_{22}^f , and G_{12}^f . If this combination turns out to be isotropic in space time we can proceed with polar coordinate decomposition. Otherwise we need to follow a tricky decomposition which we will use below for I_{22} . But, there is an interesting aspect of these second order contributions. If the second order term involves product of two different fugacities, it leads to relevant contributions only if the combinations of the fields are contracted at the same space-time point which renormalizes other fugacities. This aspect simplifies the calculation of the second terms involving product of two different fugacities.

For illustrative purposes of the above procedures first we will pick I_{11} .

$$\begin{aligned} I_{11} &= \frac{y_1^2}{2a^4} \int_{\vec{R}, \vec{r}} \langle e^{i2\pi[\phi_1(\vec{R}+\vec{r}/2)+\phi_1(\vec{R}-\vec{r}/2)]} + \text{c.c.} \\ &\quad + e^{i2\pi[\phi_1(\vec{R}+\vec{r}/2)-\phi_1(\vec{R}-\vec{r}/2)]} + \text{c.c.} \rangle^f \\ &= \frac{y_1^2}{a^4} e^{-4\pi^2 G_{11}^f(0)} \int_{\vec{R}, \vec{r}} [(e^{-4\pi^2 G_{11}^f(\vec{r})} - 1) \\ &\quad \times \cos\{2\pi[\phi_1(\vec{R}+\vec{r}/2) + \phi_1(\vec{R}-\vec{r}/2)]\} + (e^{4\pi^2 G_{11}^f(\vec{r})} - 1) \\ &\quad \times \cos\{2\pi[\phi_1(\vec{R}+\vec{r}/2) - \phi_1(\vec{R}-\vec{r}/2)]\}]. \quad (\text{A10}) \end{aligned}$$

First integral generates higher harmonic $\cos[4\pi\phi_1(\vec{R})]$ from the first integral range of the relative coordinate. The same integral in the second integral range generates a term proportional to the higher harmonic multiplied by the square of the gradient of the field ϕ_1 . So, obviously, all these terms are irrelevant. Relevant contribution comes from the second integral when we concentrate on the second integral range of the relative coordinate. After a gradient expansion for cosine term we obtain

$$I_{11} \approx -\frac{A_1}{2} y_1^2 \int d\vec{x} (\nabla\phi_1)^2. \quad (\text{A11})$$

A_1 is a regularization dependent constant which in our case is $4\pi^3$. This will contribute to the renormalization of J . Now we will pick a cross term, e.g.,

$$\begin{aligned} I_{12} &= \frac{y_1 y_2}{2a^4} \int_{\vec{R}, \vec{r}} \langle e^{i[2\pi\phi_1(\vec{R}+\vec{r}/2)+2\pi\phi_2(\vec{R}-\vec{r}/2)]} + \text{c.c.} \\ &\quad + e^{i[2\pi\phi_1(\vec{R}+\vec{r}/2)-2\pi\phi_2(\vec{R}-\vec{r}/2)]} + \text{c.c.} \rangle^f \\ &= \frac{y_1 y_2}{a^4} e^{-2\pi^2[G_{11}^f(0)+G_{22}^f(0)]} \int_{\vec{R}, \vec{r}} \{(e^{-4\pi^2 G_{12}^f(\vec{r})} - 1) \\ &\quad \times \cos[2\pi\phi_1(\vec{R}+\vec{r}/2) + 2\pi\phi_2(\vec{R}-\vec{r}/2)] + (e^{4\pi^2 G_{12}^f(\vec{r})} - 1) \\ &\quad \times \cos[2\pi\phi_1(\vec{R}+\vec{r}/2) - 2\pi\phi_2(\vec{R}-\vec{r}/2)]\}. \quad (\text{A12}) \end{aligned}$$

As mentioned above here we have to deal with only an isotropic propagator G_{12}^f and hence polar coordinate will be useful. From the first range of the \vec{r} integral we will get the contribution

$$\begin{aligned} I_{12} &\approx \left(\frac{y_1 y_2}{a^2} \right) e^{-2\pi^2[G_{11}^f(0)+G_{22}^f(0)]} [\pm 4\pi^2 G_{12}^f(0)] \\ &\quad \times \int_{\vec{R}} \cos[2\pi\phi_1(\vec{R}) \mp 2\pi\phi_1(\vec{R})] \quad (\text{A13}) \end{aligned}$$

which renormalizes y_\pm . In the second range of the integrals we will do a gradient expansion for the cosine terms which leads to the contributions proportional to $\cos[2\pi\phi_1(\vec{R}) \pm 2\pi\phi_2(\vec{R})] \times (\nabla_R\phi_1 \mp \nabla_R\phi_2)^2$. After Fourier transformation this leads to the terms which are combinations of frequency or momentum with cosine and hence irrelevant.

Two interesting second order terms are I_{1+} and I_{1-} . For the relevant part of these terms we get

$$\begin{aligned} I_{1+} &\approx \frac{y_1(l)y_+(l)}{a^4} e^{-2(1+1/z)l} \int_{\vec{R}, \vec{r}} (e^{4\pi^2[G_{11}^f(\vec{r})+G_{12}^f(\vec{r})]} - 1) \\ &\quad \times \cos[2\pi\phi_1(\vec{R}-\vec{r}/2) + 2\pi\phi_2(\vec{R}-\vec{r}/2) \\ &\quad - 2\pi\phi_1(\vec{R}+\vec{r}/2)], \\ I_{1-} &\approx \frac{y_1(l)y_-(l)}{a^4} e^{-2(1+1/z)l} \int_{\vec{R}, \vec{r}} (e^{4\pi^2[G_{11}^f(\vec{r})-G_{12}^f(\vec{r})]} - 1) \\ &\quad \times \cos[2\pi\phi_1(\vec{R}+\vec{r}/2) + 2\pi\phi_2(\vec{R}-\vec{r}/2) \\ &\quad - 2\pi\phi_1(\vec{R}-\vec{r}/2)]. \quad (\text{A14}) \end{aligned}$$

Recalling that $G_{11}^f + G_{12}^f = 0$ we can see that the relevant part of I_{1+} vanishes identically. As both G_{11}^f and G_{12}^f are isotropic in space time polar decomposition is valid for I_{1-} . Finally we get

$$I_{1-} \approx \frac{y_1 y_-}{a^2} 4\pi J l \int d\vec{x} \cos(2\pi\phi_2). \quad (\text{A15})$$

I_{11} , I_{12} , I_{1+} , and I_{1-} exhaust all the second order terms that involve the fugacity y_1 . Now we will also exhaust all the second order terms that involve the fugacity y_2 . For the relevant part of I_{2+} and I_{2-} we get

$$\begin{aligned} I_{2+} &\approx \frac{y_2(l)y_+(l)}{a^4} e^{-2(1+1/z)l} \int_{\vec{R}, \vec{r}} (e^{4\pi^2[G_{22}^f(\vec{r})+G_{12}^f(\vec{r})]} - 1) \\ &\quad \times \cos[2\pi\phi_1(\vec{R} - \vec{r}/2) + 2\pi\phi_2(\vec{R} - \vec{r}/2) \\ &\quad - 2\pi\phi_2(\vec{R} + \vec{r}/2)], \\ I_{2-} &\approx \frac{y_2(l)y_-(l)}{a^4} e^{-2(1+1/z)l} \int_{\vec{R}, \vec{r}} (e^{4\pi^2[G_{22}^f(\vec{r})-G_{12}^f(\vec{r})]} - 1) \\ &\quad \times \cos[2\pi\phi_2(\vec{R} + \vec{r}/2) + 2\pi\phi_1(\vec{R} - \vec{r}/2) \\ &\quad - 2\pi\phi_2(\vec{R} - \vec{r}/2)]. \end{aligned} \quad (\text{A16})$$

Both of the combinations $G_{22}^f(\vec{r}) \pm G_{12}^f(\vec{r})$ involve the anisotropic part of the propagator G_{22}^f . Since the relevant contributions from the two terms above will come from the contraction of the fields at the same space-time point we can set $\vec{r}=0$ without further difficulty and obtain

$$I_{2+} \approx \frac{y_2 y_+}{a^2} 2\alpha l \int d\vec{x} \cos(2\pi\phi_1),$$

$$I_{2-} \approx \frac{y_2 y_-}{a^2} 2(\alpha + 2\pi J) l \int d\vec{x} \cos(2\pi\phi_1). \quad (\text{A17})$$

Finally we consider I_{22} which will exhaust all the terms that involve y_2 .

$$\begin{aligned} I_{22} &= \frac{y_2^2}{a^4} e^{-4\pi^2 G_{22}^f(0)} \int_{\vec{R}, \vec{r}} \{(e^{-4\pi^2 G_{22}^f(\vec{r})} - 1) \\ &\quad \times \cos[2\pi\phi_2(\vec{R} + \vec{r}/2) + 2\pi\phi_2(\vec{R} - \vec{r}/2)] \\ &\quad + (e^{4\pi^2 G_{22}^f(\vec{r})} - 1) \cos[2\pi\phi_2(\vec{R} + \vec{r}/2) - 2\pi\phi_2(\vec{R} - \vec{r}/2)]\}. \end{aligned} \quad (\text{A18})$$

Regardless of the anisotropic interaction the first integral leads to higher harmonics of ϕ_2 and hence can be ignored. Calculation of the second integral is tricky but leads to contributions involving $(\partial_x \phi_2)^2$ and $(\partial_x \phi_2)^2$. But, in the original action such terms are not present and these are also of higher order than $|\omega||\phi_2|^2$ and hence irrelevant. Though the second integral produces irrelevant terms we will describe the way to calculate it as such a calculation will be required later on for I_{--} . We will break the integral into two parts corresponding to only onsite contraction and offsite contraction of the field ϕ_2 .

$$\begin{aligned} I_{22} &\approx \frac{y_2^2}{a^4} e^{-4\pi^2 G_{22}^f(0)} \int_{\vec{R}, \vec{r}} (e^{4\pi^2 G_{22}^f(\vec{r})} - 1) \cos[2\pi\phi_2(\vec{R} + \vec{r}/2) - 2\pi\phi_2(\vec{R} - \vec{r}/2)] \\ &= \frac{y_2^2}{a^3} e^{-4\pi^2 G_{22}^f(0)} \int dx du d\tau (e^{4\pi^2 G_{22}^f(0, \tau)} - 1) \cos[2\pi\phi_2(x, u + \tau/2) - 2\pi\phi_2(x, u - \tau/2)] \\ &\quad + \frac{y_2^2}{a^4} e^{-4\pi^2 G_{22}^f(0)} \int_{\vec{R}, \vec{r}} (e^{4\pi^2 G_{22}^f(l, \vec{r})} - 1) \cos[2\pi\phi_2(\vec{R} + \vec{r}/2) - 2\pi\phi_2(\vec{R} - \vec{r}/2)] \\ &\quad - \frac{y_2^2}{a^3} e^{-4\pi^2 G_{22}^f(0)} \int dx du d\tau (e^{4\pi^2 G_{22}^f(0, \tau)} - 1) \cos[2\pi\phi_2(x, u + \tau/2) - 2\pi\phi_2(x, u - \tau/2)], \end{aligned} \quad (\text{A19})$$

where $u = \frac{\tau_1 + \tau_2}{2}$ and $\tau = \tau_2 - \tau_1$. We have also broken G_{22}^f into two parts G_{22}^{fI} and G_{22}^{fA} corresponding to isotropic and anisotropic interactions, respectively. Rearrangement of I_{22} in this form has been used previously by Bobbert *et al.*²⁸ For the first and third integrals which involve only onsite contraction we can break up the integrals into three parts

$$\int d\tau = \int_0^a d\tau + \int_a^{ae^l} d\tau + \int_{ae^l}^\infty d\tau. \quad (\text{A20})$$

The second range of the integrals contribute terms proportional to $(\partial_u \phi_2)^2$. It turns out that the contributions from the first and third integrals cancel each other. Second integral

involves only isotropic function of $|\vec{r}|$ and we can use polar coordinates as mentioned above which will contribute a term proportional to $(\nabla_R \phi_2)^2$.

Finally we have to consider only two other second order terms I_{++} and I_{--} . The relevant part of these is given by

$$\begin{aligned} I_{++} &\approx \frac{y_+^2(l)}{a^4} e^{-2(1+1/z)l} \int_{\vec{R}, \vec{r}} (e^{4\pi^2[G_{11}^f(\vec{r})+G_{22}^f(\vec{r})+2G_{12}^f(\vec{r})]} - 1) \\ &\quad \times \cos\{2\pi[\phi_1(\vec{R} + \vec{r}/2) + \phi_2(\vec{R} + \vec{r}/2) - \phi_1(\vec{R} - \vec{r}/2) \\ &\quad - \phi_2(\vec{R} - \vec{r}/2)]\}, \end{aligned}$$

$$I_{--} \approx \frac{y_-^2(l)}{a^4} e^{-2(1+1/z)l} \int_{\vec{R}, \vec{r}} (e^{4\pi^2[G_{11}^f(\vec{r})+G_{22}^f(\vec{r})-2G_{12}^f(\vec{r})] - 1}) \\ \times \cos\{2\pi[\phi_1(\vec{R} + \vec{r}/2) - \phi_2(\vec{R} + \vec{r}/2) - \phi_1(\vec{R} - \vec{r}/2) \\ + \phi_2(\vec{R} - \vec{r}/2)]\}, \quad (\text{A21})$$

$G_{11}^f(\vec{r}) + G_{22}^f(\vec{r}) + 2G_{12}^f(\vec{r}) = \delta(x) \frac{\alpha}{\pi^2} K_0(\lambda \sqrt{\tau^2 + a^2})$ which depends only on time. This implies for I_{++} the relevant contribution is obtained by contracting the combination of the fields $\phi_1 + \phi_2$ at the same spatial point but at different times. So, we need to integrate over only $\tau = \tau_2 - \tau_1$. After breaking up the integral into three parts as we have done before the relevant contribution will come from the second range of the integral and we obtain

$$I_{++} \approx -\frac{A_+}{2} y_+^2 \int d\vec{x} (\partial_\tau \phi_1)^2. \quad (\text{A22})$$

A_+ is a regularization dependent constant and for the regularization used above, $A_+ = 4\pi^2$. We have ignored the irrelevant terms like $(\partial_\tau \phi_2)^2$ and $\phi_1 \phi_2$ involving spatial or temporal derivatives.

Since $G_{11}^f(\vec{r}) + G_{22}^f(\vec{r}) + 2G_{12}^f(\vec{r})$ involves both isotropic and anisotropic parts, the evaluation of I_{--} is more complicated. But, we can carry out the calculation using the trick mentioned above for I_{22} . Ignoring irrelevant contributions we get

$$I_{--} \approx -\frac{A_-}{2} y_-^2 \int d\vec{x} (\nabla \phi_1)^2, \quad (\text{A23})$$

where A_- is another regularization dependent constant and for the regularization method chosen above $A_- = 4\pi^3$.

Since we are integrating out the momenta for a fixed frequency shell, the coefficient of $\int d\vec{x} (\partial_\tau \phi_1)^2$ has to be kept fixed. Due to this reason after collecting the second order terms involving $\int d\vec{x} (\partial_\tau \phi_1)^2$ and rescaling the space-time coordinates we obtain

$$\frac{1}{J'} = e^{(1/z-1)l} \left[\frac{1}{J} + (A_1 y_1^2 + A_+ y_+^2 + A_- y_-^2) l \right], \quad (\text{A24})$$

which leads to

$$\frac{dJ}{dl} = J \left[\left(1 - \frac{1}{z} \right) - J(A_1 y_1^2 + A_+ y_+^2 + A_- y_-^2) \right]. \quad (\text{A25})$$

The anisotropic scaling prescription $k \rightarrow k e^{-l/z}$ can be used to keep the coefficient of k^2 fixed and $1/z$ is determined by the difference of the coefficients of the terms involving $\int d\vec{x} (\partial_\tau \phi_1)^2$ and $\int d\vec{x} (\partial_x \phi_1)^2$ generated at the second order RG transformation. This trick to extract the dynamic exponent in a perturbative analysis is well-known.⁵⁰ Following this trick we get

$$2 \left(1 - \frac{1}{z} \right) = A_+ y_+^2. \quad (\text{A26})$$

This completes the derivation of the recursion relations of the coupling constants up to the second order.

-
- ¹S. Chakravarty, Phys. Rev. Lett. **49**, 681 (1982).
²A. J. Bray and M. A. Moore, Phys. Rev. Lett. **49**, 1545 (1982).
³S. Sachdev, *Quantum Phase Transition* (Cambridge University Press, Cambridge, England, 1999).
⁴A. Schmid, Phys. Rev. Lett. **51**, 1506 (1983).
⁵S. Coleman, *Aspects of Symmetry* (Cambridge University Press, Cambridge, England, 1985).
⁶A. Caldeira and A. Leggett, Ann. Phys. (N.Y.) **149**, 374 (1983); **153**, 445(E) (1984).
⁷L.-D. Chang and S. Chakravarty, Phys. Rev. B **29**, 130 (1984); **30**, 1566(E) (1984).
⁸P. W. Anderson, Phys. Rev. Lett. **18**, 1049 (1967).
⁹A. Kapitulnik, N. Mason, S. A. Kivelson, and S. Chakravarty, Phys. Rev. B **63**, 125322 (2001).
¹⁰S. Han, J. Lapointe, and J. E. Lukens, Phys. Rev. Lett. **66**, 810 (1991).
¹¹J. S. Penttilä, Ü. Parts, P. J. Hakonen, M. A. Paalanen, and E. B. Sonin, Phys. Rev. Lett. **82**, 1004 (1999).
¹²P. Werner and M. Troyer, Phys. Rev. Lett. **95**, 060201 (2005).
¹³A. Bezryadin, M. Tinkham, and C. N. Lau, Nature (London) **404**, 971 (2000).
¹⁴C. N. Lau, N. Markovic, M. Bockrath, A. Bezryadin, and M. Tinkham, Phys. Rev. Lett. **87**, 217003 (2001).
¹⁵A. Rogachev and A. Bezryadin, Appl. Phys. Lett. **83**, 512 (2003).
¹⁶A. T. Bollinger, A. Rogachev, M. Remeika, and A. Bezryadin, Phys. Rev. B **69**, 180503(R) (2004).
¹⁷M. L. Tian, J. G. Wang, J. S. Kurtz, Y. Liu, M. H. W. Chan, T. S. Mayer, and T. E. Mallouk, Phys. Rev. B **71**, 104521 (2005).
¹⁸S. Chakravarty, G.-L. Ingold, S. Kivelson, and A. Luther, Phys. Rev. Lett. **56**, 2303 (1986).
¹⁹S. Chakravarty, G. L. Ingold, S. Kivelson, and G. Zimanyi, Phys. Rev. B **37**, 3283 (1988).
²⁰M. P. A. Fisher, Phys. Rev. Lett. **57**, 885 (1986).
²¹M. P. A. Fisher, Phys. Rev. B **36**, 1917 (1987).
²²B. G. Orr, H. M. Jaeger, A. M. Goldman, and C. G. Kuper, Phys. Rev. Lett. **56**, 996 (1986); **56**, 378 (1986).
²³A. M. Goldman, Physica E (Amsterdam) **18**, 1 (2003).
²⁴A. J. Rimberg, T. R. Ho, C. Kurdak, J. Clarke, K. L. Campman, and A. C. Gossard, Phys. Rev. Lett. **78**, 2632 (1997).
²⁵Y. Takahide, R. Yagi, A. Kanda, Y. Ootuka, and S.-I. Kobayashi, Phys. Rev. Lett. **85**, 1974 (2000).
²⁶H. Miyazaki, Y. Takahide, A. Kanda, and Y. Ootuka, Phys. Rev. Lett. **89**, 197001 (2002).
²⁷S. Panyukov and A. Zaikin, Phys. Lett. A **156**, 119 (1991).
²⁸P. A. Bobbert, R. Fazio, G. Schön, and A. D. Zaikin, Phys. Rev. B **45**, 2294 (1992).
²⁹P. A. Bobbert, R. Fazio, G. Schön, and G. T. Zimanyi, Phys. Rev. B **41**, 4009 (1990).
³⁰S. E. Korshunov, Europhys. Lett. **9**, 107 (1989).
³¹S. E. Korshunov, Sov. Phys. JETP **68**, 609 (1989).
³²W. Zwerger, Europhys. Lett. **9**, 421 (1989).
³³W. Zwerger, Z. Phys. B: Condens. Matter **78**, 111 (1990).

- ³⁴S. Tewari, J. Toner, and S. Chakravarty, Phys. Rev. B **72**, 060505 (2005).
- ³⁵S. Tewari, J. Toner, and S. Chakravarty, Phys. Rev. B **73**, 064503 (2006).
- ³⁶G. Refael, E. Demler, Y. Oreg, and D. S. Fisher, Phys. Rev. B **68**, 214515 (2003).
- ³⁷H. A. Fertig and K. Majumdar, Ann. Phys. **305**, 190 (2003).
- ³⁸S. Pankov, S. Florens, A. Georges, G. Kotliar, and S. Sachdev, Phys. Rev. B **69**, 054426 (2004).
- ³⁹A. Gamba, M. Grilli, and C. Castellani, Nucl. Phys. B **556**, 463 (1999).
- ⁴⁰S. Sachdev, P. Werner, and M. Troyer, Phys. Rev. Lett. **92**, 237003 (2004).
- ⁴¹H. P. Büchler, V. B. Geshkenbein, and G. Blatter, Phys. Rev. Lett. **92**, 067007 (2004).
- ⁴²A. D. Zaikin, D. S. Golubev, A. van Otterlo, and G. T. Zimanyi, Usp. Fiz. Nauk **168**, 244 (1998) [Phys. Usp. **42**, 226 (1998)].
- ⁴³M. V. Feigelman and A. I. Larkin, Chem. Phys. **235**, 107 (1998).
- ⁴⁴B. Spivak, A. Zyuzin, and M. Hruska, Phys. Rev. B **64**, 132502 (2001).
- ⁴⁵J. E. Mooij and G. Schön, Phys. Rev. Lett. **55**, 114 (1985).
- ⁴⁶A. D. Zaikin, D. S. Golubev, A. van Otterlo, and G. T. Zimanyi, Phys. Rev. Lett. **78**, 1552 (1997).
- ⁴⁷S. Khlebnikov and L. P. Pryadko, Phys. Rev. Lett. **95**, 107007 (2005).
- ⁴⁸J. B. Kogut, Rev. Mod. Phys. **51**, 659 (1979).
- ⁴⁹T. Ohta and D. Jasnow, Phys. Rev. B **20**, 139 (1979).
- ⁵⁰A. Vishwanath, J. E. Moore, and T. Senthil, Phys. Rev. B **69**, 054507 (2004).